Characterization of New H-Bonded Liquid Crystalline Complexes Based on Iminophenyl Nicotinate

Rua B. Alnoman [1], Mohamed Hagar [1,2,*], Hoda A. Ahmed [3,*], Khulood A. Abu Al-Ola [4], Magdi M. Naoum [3], Fahad Al-Elati [1], Yousef Abdullah Zaid [1], Abdulrahman Alsharif [1], Yazeed Al-Juhani [1] and Abdulmjeed Abulrhelh [1]

1   Chemistry Department, College of Sciences, Yanbu, Taibah University, Yanbu 30799, Saudi Arabia; rua-b-n@live.co.uk (R.B.A.); tu3702238@taibahu.edu.sa (F.A.-E.); tu3701218@taibahu.edu.sa (Y.A.Z.); tu3706375@taibahu.edu.sa (A.A.); yazed2543@taibahu.edu.sa (Y.A.-J.); Jedo1416@gmail.com (A.A.)
2   Chemistry Department, Faculty of Science, Alexandria University, Alexandria 21321, Egypt
3   Department of Chemistry, Faculty of Science, Cairo University, Cairo 12613, Egypt; magdinaoum@yahoo.co.uk
4   Chemistry Department, College of Sciences, Al-Madina Al-Munawarah, Taibah University, Al-Madina 30002, Saudi Arabia; Kabualola@taibahu.edu.sa
*   Correspondence: mhagar@taibahu.edu.sa (M.H.); ahoda@sci.cu.edu.eg (H.A.A.)

check for updates

Abstract: Two new 1:2 supramolecular H-bonded liquid crystalline complexes (SMHBCs) were prepared through double H-bond interactions between either isophthalic acid (A) or terephthalic acid (B) and a nicotinate Schiff base (I6). The formed complexes were thermally investigated by differential scanning calorimetry (DSC), and their phases were identified by polarized optical microscopy (POM) and UV-spectroscopy. The formation of 1:2 hydrogen-bonded complexes was confirmed through their Fermi-bands observed by FT-IR spectroscopy. The first system (I6/A) was found to possess enantiotropic smectic A and nematic mesophases. Induced broad range of smectic A phase was observed in **I6/A** complex which is not shown by their individual components. The second complex system (I6/B) was purely nematogenic. Density functional theory (DFT) calculations were applied to predict their geometrical parameters. Theoretical studies revealed that the isophthalic complex adopted the W-shape; while the U-shape was adopted by the terephthalic acid complex (I6/B). The linear geometry of the complex based on the isophthalic acid enhanced the mesomorphic behavior observed by the terephthalic complex; I6/B. Actually; the orientation of the two carboxylic groups was shown to highly affect the softness of the derived complex. On the other hand; the mapping orientation of the charge distribution can be used to explain the mesophase behavior. The photophysical characterization of isophthalic complex (I6/A) is also discussed

Keywords: dicarboxylic acid supramolecular H-bonding complexes; mesomorphic behavior; induced phase; molecular geometry; DFT calculations; photophysical studies

1. Introduction

The design of the supramolecular hydrogen bonded complex (SMHBC) molecular structures actually helps to achieve the required mesophases necessary for special applicable trends [1]. Hydrogen bond interactions are based on two functional groups that are controlled by two components: an electron-acceptor and an electron-donor.

Generally, the mesomorphic behavior of an organic compound is basically dependent on its molecular architecture, whereby a small change in its molecular shape leads to a considerable change in its mesomorphic behavior [2]. Thus, the preparation of a photosensitive supramolecular liquid

crystal (SMLCs) through intermolecular H-bond interactions is one interesting area of research [3–9]. The photosensitive phenomenon is considered to be one of the research domains that, under incident light, induces order and/or disorder between mesomorphic molecules [10–12].

The design of a liquid crystalline molecule containing a double bond, as an additional linking group within its molecular formula, brings about special features. Thus, introducing a double bond within a molecule enables a non-mesomorphic compound to be mesomorphic [13], as well as the possibility of photoisomerization in its liquid crystalline phases [12,14]. A Schiff base (CH=N) linking group provides a stepped core structure and a higher stability of the prepared materials that affects the observed mesophases [15]. On the other hand, the addition of heterocyclic rings with electronegative hetero-atoms definitely influences and impacts the polar induction power of a compound [16]. The use of dinitrogen heterocyclic rings with different orientations of the two nitrogen atoms widely improves the mesomorphic properties of SMLC complexes [17–19].

Kato et.al. [20] investigated the mesophase behavior of the hydrogen-bonded supramolecular complexes of isophthalic acid with trans-4-alkoxy-4'-stilbazole. Since 2004, hydrogen bonding has also been used to design angular liquid crystals [3,21]. The mutual effect of several optical parameters needs stimulated data about the energy gaps between the frontier molecular orbitals, as well as their molecular structure.

Recently, our research group has centered its attention on the computational estimations of new synthesized SMHBLC materials to experimentally illustrate their mesomorphic behavior in terms of theoretical calculations [4,22–24]. These studies have been focused on the correlation between the mesomorphic transition data and the evaluated computational calculations for SMHBCs. Another type of H-bonding assembly is the angular- shaped complexes, as interaction of 1:2 of phthalic acid and stilbazole derivatives [20]. In this case, both individual components are non-mesomorphic, whereas their H-bonded complexes show induced nematic mesophases [20]. The geometrical conformations of SMHBCs depend on their molecular shapes that play an important role on the stability and enhancement of their mesophases.

Recently, it has been observed that the possible orientation of hetero-atoms in pyridines results in the modification of the existing functions, thus introducing a new geometrical characteristic to the organic molecule [19,25]. On the other hand, the mesogenic core, flexible chains and terminal substituents play important roles in the formation, stability, type, and mesomorphic temperature range of LC compounds. The molecules in the mesophase tend to be more oriented in a parallel arrangement as the length of the terminal substituent increases [26]. In addition, the terminal chains influence the heliconical and twist–bend nematic phases [27,28].

In order to further understand the structure–property relationship of SMHBCs based on nicotinate derivatives, two series of di-pyridine derivative H-bonded complexes (1:2) have been investigated [19,25,29]. In another investigation, the 1:1 SMHBCs formed between a nitrogen atom of a Schiff base of phenyl nicotinate derivative and 4-alkoxybenzoic acids [30] were prepared and characterized. Recently, it was reported [31] that the mesomorphic properties and geometrical predictions are differently affected upon the replacement of the azo linking group in the nicotinate base derivative instead of azomethine one [30]. These results have encouraged us to extend our investigation towards the formation and characterization of other SMHBCs based on the nematogenic Schiff base nicotinate derivative (I6).

Combinations between the computational predictions of geometrical parameters with experimental findings also are important [4,9,23,25,30–34]. Recently, the great potential of LCs to be used as sensors and in bio-applications was reported [35,36].

Our present study deals with the synthesis of new supramolecular H-bonding liquid crystalline complexes based on the H-bonding interactions between two components, namely a Schiff base nicotinate derivative (I6) and either of the dibasic proton donors—isophthalic acid (A) or terephthalic acid (B). The H-bonded mixtures were prepared from one mole of the electron-acceptor A (or B) and two moles of the electron-donor I6. The study aimed to investigate the effect of geometrical orientation

of the two ester COO groups of the two isomeric complexes on their mesomorphic and optical behavior. The estimation of their geometrical parameters was done via DFT calculations. It was also aimed at relating their mesomorphic behavior with their predicted calculated thermal and structural values.

2. Experimental

The synthetic method of base 4-(4-(hexyloxyphenyliminomethyl) phenyl nicotinate I6 [30] is given as supplementary materials.

2.1. Preparation of 2:1 SMHB Complexes

The supramolecular complexes I6/A and I6/B were formed from a 2:1 molar ratio of 4-(4-(hexyloxyphenyliminomethyl) phenyl nicotinate (I6) (Aldrich, Wisconsin, WI, USA) and individually with both isophthalic acid (A) and terephthalic acid (B). The solid mixtures of the two components were melted with stirring to form an intimate blend, which was then allowed to cool to room temperature (Scheme 1). The formation of SMHBCs confirmed via differential scanning calorimetry (DSC, New Castle, DE, USA) investigations and FT-IR spectroscopy (FTIR, Nicolet iS 10 Thermo Scientific, Waltham, MA, USA).
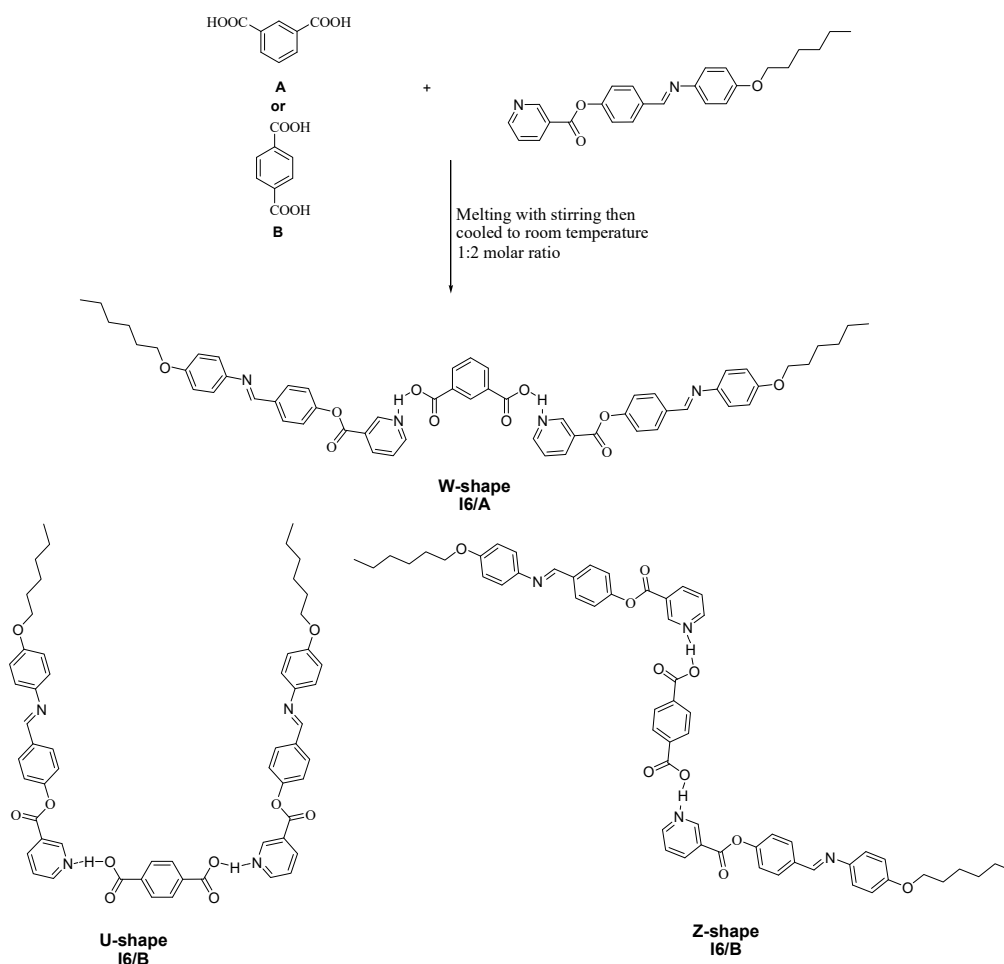
Scheme 1. Formation of the supramolecular hydrogen bonded complexes (SMHBs) I6/A and I6/B.

2.2. Computational Method for Calculations

The theoretical calculations were carried out via the Gaussian 09 software [37]. The DFT/B3LYP method and the 6-31G (d,p) basis set were selected for calculations. The geometries were optimized by minimizing the energies with respect to all geometrical parameters without imposing any molecular

symmetry constraints. The structures of the optimized geometries were drawn with Gauss View [38]. One conformer was considered for the complex derived from isophthalic acid I6/A, and two conformers for the other complex, I6/B. The selection of these conformers was based on the steric hindrance point of view.

3. Results and Discussion

3.1. FT-IR Confirmation of SMHB Complexes

The formation of the H-bonding could be estimated with many spectroscopic tools such as NMR, single crystal X-ray diffraction analysis, and FT-IR spectroscopy [19,31,39,40]. Here, the FT-IR stretching comparisons were reported in the crystalline state at room temperature to give excellent evidence for H-bonding formation through the appearance of three new Fermi resonance vibration bands assigned to the H-bonded OH groups of the A-, B-, and C-types [30,31,41–47]. FT-IR spectral data were recorded for the individual components, as well as for their supramolecular complexes; see Figure 1. The FT-IR spectra of I6 and A and their I6/A complex showed a band at 1728 cm^{-1} due to the C=O group of the ester moiety of the nicotinate group of the I6/A complex instead of 1743 cm^{-1} for its free base I6. The intermolecular dimeric H-bond of the carboxylic groups of the acids was replaced with that between the isophthalic acid (A) and the pyridine of the base (I6). Moreover, the A-type Fermi band of the I6/A complex lay between 3067 and 3081 cm^{-1}. Furthermore, the peaks at 2452 (I6/A) and 2363 cm^{-1} (I6/B) were assigned to B-type of the in-plane bending vibration of the O–H group. On the other hand, bands at 1902 and 1910 cm^{-1} corresponded to the C-type Fermi band for I6/A and I6/B, respectively. This was ascribed to the interaction between the overtone of the torsional effect and the fundamental stretching vibration of the OH group.
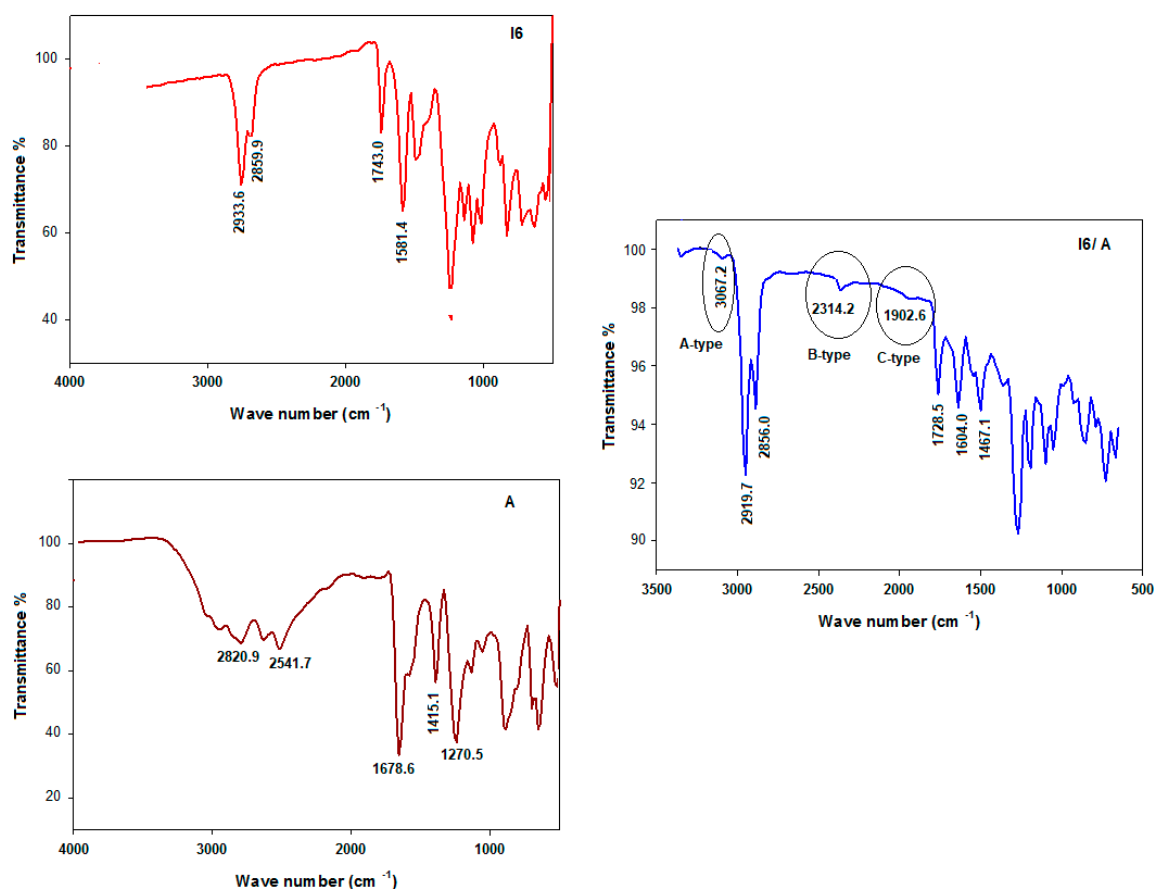

Figure 1. FT-IR spectra of the base (**I6**), isophthalic acid (**A**) and their SMHBCs (**I6/A**).

3.2. Mesomorphic and Optical Studies

The mesomorphic activities of the individual components (I6) and their 2:1 supramolecular H-bonded systems (I6/A and I6/B) were investigated. The transition temperatures (*T*) and their associated enthalpy (Δ*H*), as well as the normalized entropies (Δ*S/R*) of mesophase transitions for the investigated base (phenyl nicotinate; I6) and its SMHBCs, as derived from DSC, are collected in Table 1. It should be mentioned here that, the nicotinate derivative I6 is purely nematogenic, as it only possesses the nematic phase, whereas the terephthalic and isophthalic acids are non-mesomorphic. Polarized optical microscopy (POM) textures of the analyzed I6/A and I6/B complexes are presented in Figure 2. In order to ensure the stability of the mixtures, the DSC measurements were performed for two heating–cooling cycles. All thermal analyses of these complexes were recorded from the second heating scan. DSC measurements were confirmed by the POM texture observations. As can be seen in Table 1 and Figure 2, the two prepared SMHBCs were mesomorphic, exhibiting high thermal activates with broad range of stabilities. The DSC thermograms, upon second heating/cooling cycles, of investigated I6/A and I6/B complexes are shown in Figure 3. As shown in Figure 3, enantiotropic mesophases (mesophases observed upon heating and cooling cycles) were observed for both the I6/A and I6/B SMHB complexes. The data revealed that the 2:1 SMHB complexes possessed melting transitions lower than the individual components, where the melting temperatures of the isophthalic and terephthalic acids were 342 and 300 °C, respectively. In case of the isophthalic complex (I6/A), all investigations revealed that it was dimorphic and exhibited the smectic A phase followed by the nematic phase, meaning that an induced Smectic A (SmA) phase with a relatively wide temperature range (~43.7 °C). The range in which the nematic phase was stable was lower than the Schiff base precursor (from 53.9 °C for I6 to 16.3 °C for complex I6/A and 52.7 for complex I6/B. Moreover, the N–I transition temperature was increased to 186.9 for I6/A. In the second system, I6/B, it was observed that the 2:1 complex was slightly less stable than its isomer I6/A. Thus, the shape and core of the H-donor molecule were found to be more effective on the stability of the observed N phase. It can be concluded that the increment of the molecular anisotropy influenced the nematic phases range and its stability, thus agreeing with previous reported work [4] which stated that the increment of the mesogenic core length enhanced the nematic phase stability.

Table 1. Phase transition temperatures upon heating (T; °C), enthalpy of transitions (Δ*H*; kJ/mol), and normalized transition entropy (Δ*S/R*) of the base I6 and its supramolecular complexes, I6/A and I6/B.

System	T_{Cr-SmA}	ΔH_{Cr-SmA}	T_{Cr-N}	ΔH_{Cr-N}	T_{SmA-N}	ΔH_{SmA-N}	$\Delta S_{SmA-I}/R$	T_{N-I}	ΔH_{N-I}	$\Delta S_{N-I}/R$
I6	–	–	130.7	35.5	–	–	–	184.6	1.9	0.5
I6/A	126.9	52.8	–	–	170.6	2.3	0.6	186.9	1.0	0.3
I6/B	–	–	128.5	66.3	–	–	–	181.2	1.2	0.3

Abbreviations: Cr–SmA = solid to SmA transition; Cr–N = solid to N transition; SmA–N = SmA to N transition; and N–I = N to isotropic liquid transition.

Figure 2. Polarized optical microscopy (POM) textures of the I6/A and I6/B 2:1 SMHB complexes upon heating for: (**a**) the I6/A Smectic A (SmA) phase at 152 °C, (**b**) N phase at 179 °C, and (**c**) for I6/B N phase at 175 °C.

Figure 3. Differential scanning calorimetry (DSC) thermograms upon the second heating/cooling cycles of the 2:1 SMHB complexes with a rate 10 °C/min: (**a**) I6/A and (**b**) I6/B.

Normalized transition entropies (Table 1) were estimated for the present I6/A and I6/B 2:1 SMHBCs, and the results indicated that the variation of the entropy change could be attributed to the change in molecular interactions between individual molecules, which were accordingly affected by the polarizability and the geometrical structure of the molecule. These factors contributed to the conformational, orientational, and translational entropies of the molecule in different amounts.

The mesomorphic behavior of the I6/A complex, possessing the azomethine linkage, was compared with the previously reported corresponding azo-containing supramolecular complexes IIn/C [3]; see Scheme 2. It has been reported that IIn/C complexes adopt U-shape architectures [3] with SmA and N phases dependent on the length of the terminal alkoxy chain attached to the azo pyridine derivatives. The comparison revealed that, the present investigated isophthalic SMHBC-based Schiff base moiety (W-shape) was more stable than the previous azo-based complexes IIn/C (U-shape). Thus, it seems that the design of molecular structure or the deformation of molecular architecture could affect the formation and thermal stability of the prepared liquid crystalline compounds.

Scheme 2. SMHB IIn/C complex; where II8/C had the transitions of Cr 104.0 SmA 145.0 in isotropic liquid.

3.3. DFT Theoretical Calculations

3.3.1. Molecular Geometry of SMHBCs

The structural geometries of the prepared SMHBCs (I6/A and I6/B) were estimated by DFT theoretical calculations using B3LYP 6-311G (d,p). The absence of imaginary frequencies proved the stability of the optimized structures of all H-bonded interactions for the complexes. Figure 4 demonstrates the optimal structural geometry of the Schiff base nicotinate (I6) and its I6/A and I6/B H-bonded complexes of isophthalic acid A and terephthalic acid B.
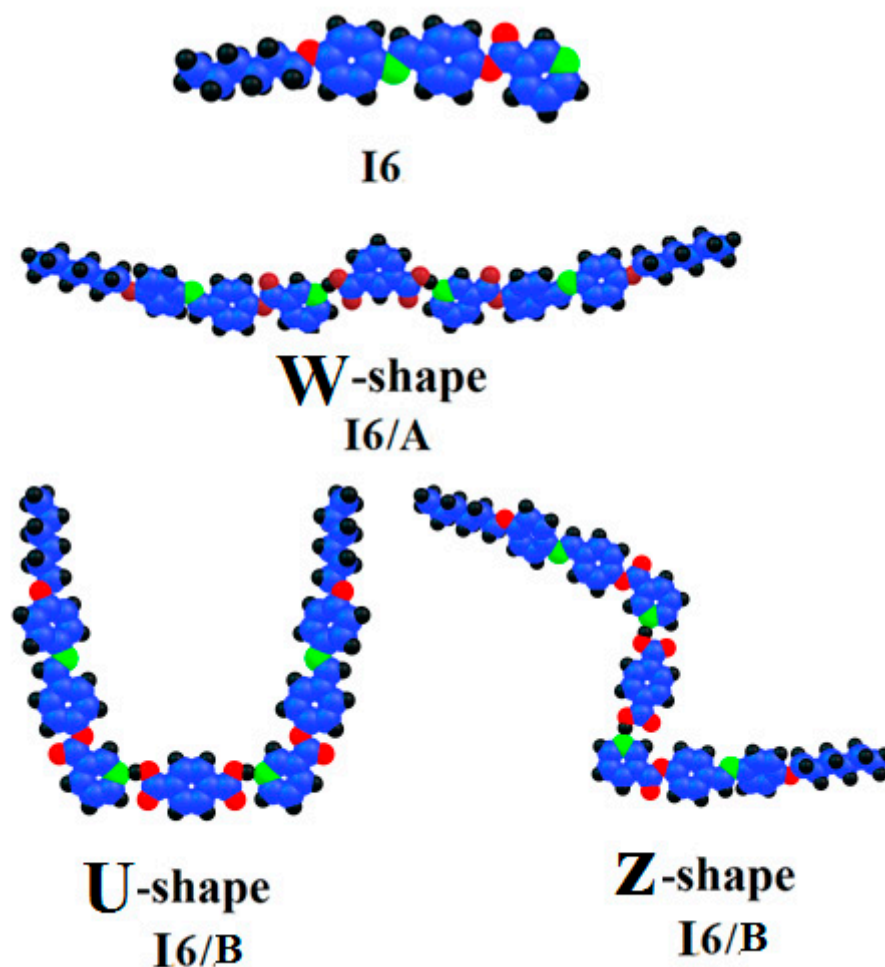
Figure 4. The calculated molecular geometry of the I6/A and I6/B SMHBCs.

Even though both acids A and B and the nicotinate base I6 were in planar geometry, their SMHBCs were neither linear nor co-planar. As seen in Figure 4, the orientation of the two carboxylic groups of phthalic acid affected the geometry and the planarity of their I6/A and I6/B H-bonded supramolecular complexes. The geometrical orientation of the two meta carboxylic groups of the isophthalic acid afforded the W-shape SMHB complex. While, its para oriented isomer may exhibit two conformers, namely, the U- and Z-shaped geometries. As can be seen in Figure 4, the SMHB complex derived from the isophthalic acid I6/A was more linear and more co-planar than its corresponding positional isomeric complex I6/B. Recently, we reported the relationship between the estimated geometry of the liquid crystalline materials and their mesomorphic behavior [9,19,25,31–34,48–50]. Since the geometry of both the SMHBCs were completely different, it could be an explanation for the presence of the smectic and short range of nematic mesophases in the more linear I6/B H-bonded complex and mesomorphic nematic phase of the complex derived from the I6/B terephthalic acid. The linear geometry of the I6/A complex of the isophthalic acid permitted a high degree of parallel interaction between the molecules and enforced the molecular packing to enhance the more ordered smectic mesophase with a wider range than that of the nematic one. However, the U-shape of the less planar and less linear facilitated the terminal aggregation rather than the lateral. Such interaction developed the formation of the less ordered nematic mesophase.

The predicted thermal parameters were estimated by applying the same method and at the same set for both I6/A and I6/B H-bonded complexes and their conformers, as well as the azomethine nicotinate base I6, and all of these data are summarized in Table 2. As is obvious from Table 2, the Z-shape of the SMHBC derived from the terephthalic acid B was less stable than its U-shape

stereoisomer; however, the low energy difference between them was evidence for their inter-conversion equilibrium. On the other hand, the U-shaped geometry of the terephthalic acid was more stable than that of the W-shaped by 1.4 kcal mol^{-1}.

Table 2. Thermal parameters (Hartree/Particle) of the I6 base, as well as the I6/A and I6/B H-bonded complex conformers.

Parameter		I6	I6/A	I6/B	
			W-shape	U-shape	Z-shape
E_{corr}		0.461893	1.054168	1.054486	1.054400
ZPVE		−1302.959331	−3215.234669	−3215.236728	−3215.236665
E_{tot}		−1302.932846	−3215.165279	−3215.167518	−3215.167424
H		−1302.931902	−3215.164335	−3215.166574	−3215.166480
G		−1303.021887	−3215.366005	−3215.366299	−3215.366334
Total μ		4.88	6.81	6.6996	11.4971
Polarizability α		356.7	836.1	830.10	830.73
Dimensions Å	Width (D)	7.9	10.7	27.9	20.4
	Length (L)	28.5	63.2	29.7	50.7
Aspect ratio (L/D)		3.6	5.9	1.1	2.5

Abbreviations; ZPVE: sum of electronic and zero-point energies; E_{tot}: sum of electronic and thermal energies; H: sum of electronic and thermal enthalpies; G: sum of electronic and thermal free energies; D: estimated width of the molecule; and L: estimated length of the molecule.

In order to investigate the impact of the space filling of the SMHB compounds on the mesomorphic behavior, the dimensional values (D width and L length) and the aspect ratios (L/D) were estimated by calculating their diameter of collision in comparison with the I6 Schiff base. Since the H-bonded complex derived from the isophthalic acid was more linear than that of the U-shape of the terephthalic acid, the aspect ratio of the former was greater than the latter—5.9 and 1.1, respectively. The larger aspect ratio and the molecular packing of the W-shape illustrated its enhancement of the more ordered smectic phase with a temperature range of ΔT = 43.7 °C. Moreover, the high degree of packing could explain the higher mesophase stability of I6/A (Tc = 186.9 °C) compared with 181.2 °C for its positional isomer of the I6/B's U-shape geometry. However, the presence of the aromatic part and the alkoxy chains of I6/B on the other side of the U-shape was an illustration of the wider nematic range of ΔT = 52.7 °C due to the terminal aggregation of the chains compared with the W-shape; its nematic temperature range was ΔT = 16.3 °C.

On the other hand, the estimated dipole moment was one of the most important explanations of the type and behavior of the formed mesophases. From Table 2, it is obvious that the predicted dipole moment of the U-shaped SMHBCs complexes was higher than its W-shaped isomer. The lower dipole moment of the W-shaped complexes could be rationalized in terms of its symmetry, as well as its linearity, compared with its I6/A isomer. However, the high dipole moment and high aspect ratio of I6 was good evidence for the nematic texture of the formed mesophase with a wide range. The higher dipole moment stabilized the interactive aggregation, thus enhancing the stability and the range of the mesophase.

Figure 5 shows the estimated plots for the highest occupied molecular orbitals (HOMOs) frontier molecular orbitals (FMOs) and lowest unoccupied molecular orbitals (LUMOs) of both prepared SMHBCs I6/A and I6/B, as well as the I6 Schiff base. As shown from the figure, it is clear that the electron densities of the sites shared in the formation of the FMOs were mainly localized on the Schiff base part for both the HOMO and LUMO. The energy difference between the frontier molecular orbitals could be used in the prediction of the ability of electron to move from the HOMO to the LUMO by the electronic excitation process. The global softness (S) = 1/ΔE was the parameter that predicted the polarizability and the sensitivity of the compounds for their photoelectric effects. The higher global softness led to a

better photoelectric sensitivity and their polarizability. As shown in Table 3, the H-bonded complex derived from the isophthalic derivative A had a lower energy gap between the FMOs than that its isomer. Consequently, the latter was harder than that of the former derived from terephthalic acid B. Moreover, such H-bonding complexation increased the softness compared to the free base I6.
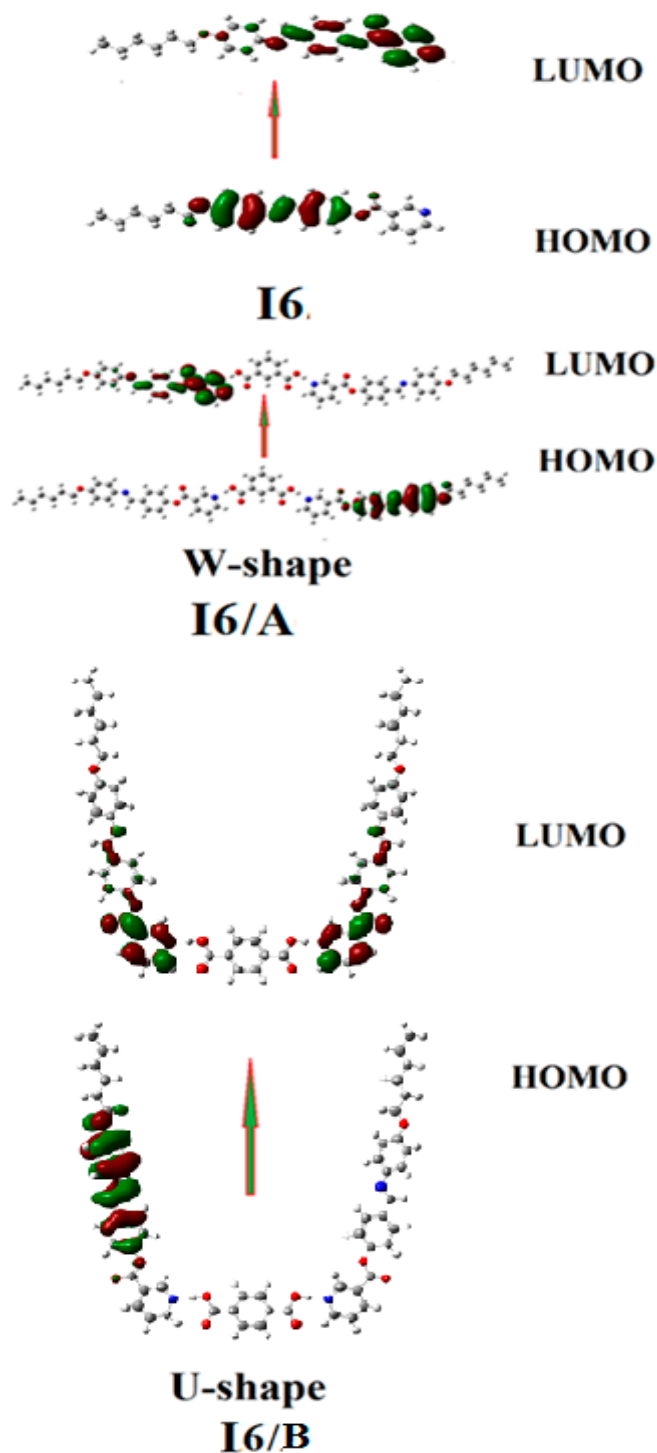

Figure 5. The estimated plots for frontier molecular orbitals of the I6/A and I6/B SMHBCs.

Table 3. Frontier molecular orbitals (FMOs) energies (a.u.), polarizability, α (Bohr^3), and dipole moment μ (Debye) of the I6 base, as well as the I6/A and I6/B SMHBCs.

Parameter	I6	I6/A	I6/B
E$_{LUMO}$	−0.08468	−0.09345	−0.09454
E$_{HOMO}$	−0.21077	−0.21429	−0.21435
ΔE$_{HOMO-LUMO}$	0.12609	0.12084	0.11981
Hardness η =0.5 * ΔE	0.06305	0.06042	0.05991
Softness S=(ΔE)$^{-1}$	7.93	8.27	8.34

3.3.2. Molecular Electrostatic Potential (MEP)

The charge distribution map for the SMHBCs of both isomers of the nicotinate base I6, I6/A, and I6/B was calculated by the same method at the same basis sets according to molecular electrostatic potential (MEP) (Figure 6). The negatively charged atomic sites (the red region) were estimated to be localized on hydrogen bonded carboxylate moiety of the alkoxy acid with little presence on the carbonyl group of the nicotinate part. Meanwhile, the moiety of the alkoxy chain was predicted to show the least negatively charged atomic sites (blue regions). As shown in Figure 6, the orientations of the dicarboxylic groups highly affected the direction and mapping of the charge distribution. Since the force of interaction between the liquid crystalline molecules depends on the mapping of the charge distribution, this could be another explanation for the nematic mesophase formation due to the terminal aggregation with the U-shape conformer compared with the symmetrical charge distribution that enhanced the parallel interaction by a high degree of the π–π aromatic stacking. On the other hand, the greater linearity of the I6/B W-shaped complexes could demonstrate the formation of the smectic texture with a broad mesomorphic range.
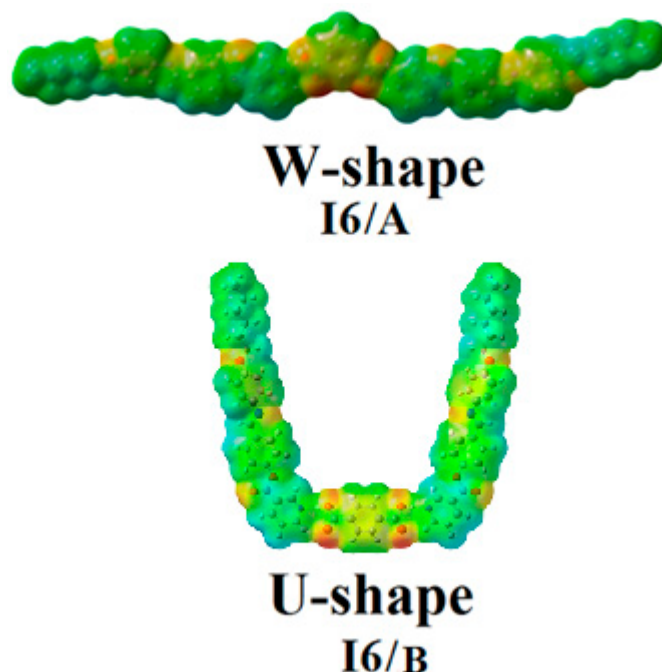
Figure 6. Molecular electrostatic potentials (MEPs) for the I6/A and I6/B SMHBCs.

3.4. Photophysical Studies

Photophysical studies of the isophthalic supramolecular complex (I6/A) were carried out by measuring UV–vis spectra in two different solvents with temperatures changes. The C = 1.8·10^{-6} mol/L of complex in Dimethyle formamide (DMF) or toluene solutions was used to record the

spectrophotometric absorption spectra bands at a temperature range of 40–100 °C. Figure 7 indicates the graphical representation of the resulted photoisomerization absorption bands. As shown in Figure 7, the I6/A SMHBC in the DMF solution had two maximum absorption bands at ~356 and ~516 nm, while in toluene, its absorption bands shifted to ~348 and ~455 nm. The absorbance slightly increased with temperature. The intense electronic delocalization and π–π* transitions of the investigated complexes, due to the presence of Schiff base linkage, were recognized as the maximum absorption in the present H-bonding interactions. Moreover, the wavelength and intensity of the absorption peak were dependent on the chromophores and the degree of conjugation that affected the absorption of light at a given wavelength. The maximum absorption bands of these complexes could be attributed to the electronic transition from the HOMO to the LUMO. Moreover, the type of the solvent affected the degree of the solvation and the type of the intermolecular interaction, consequently affecting the magnitude of the absorbance at a certain wavelength. The molar absorptivity ε in M^{-1} cm^{-1} at a given wavelength of maximum absorption was correlated as a function of temperature and is depicted in Figure 8. As can be seen in Figure 8, a linear dependency of the molar absorptivity was observed as an increment of temperature, such that it could be concluded that the shape of a given absorption peak is essentially determined by some characteristic parameters that may be evaluated from the observed spectrum at any one temperature [51].
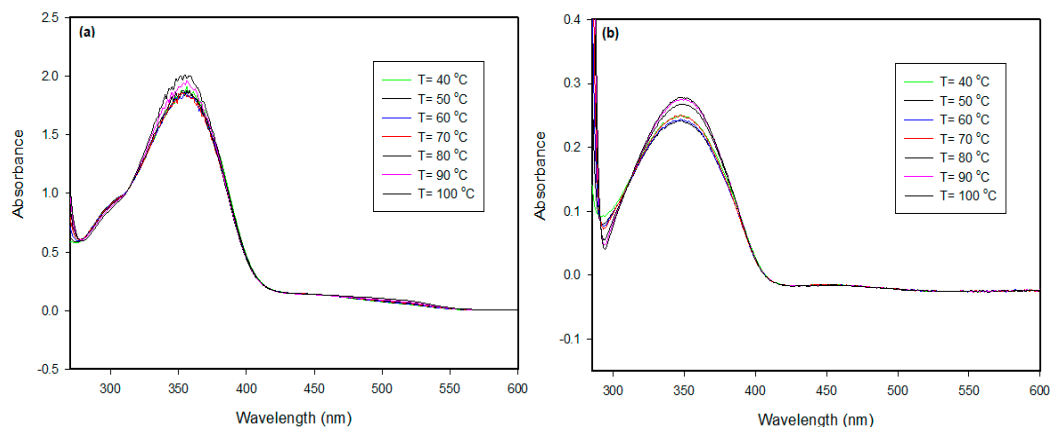

Figure 7. UV absorption spectrum of the I6/A supramolecular complex with a heating range from 40 to 100 °C (**a**) in the DMF solvent and (**b**) in the toluene solvent.
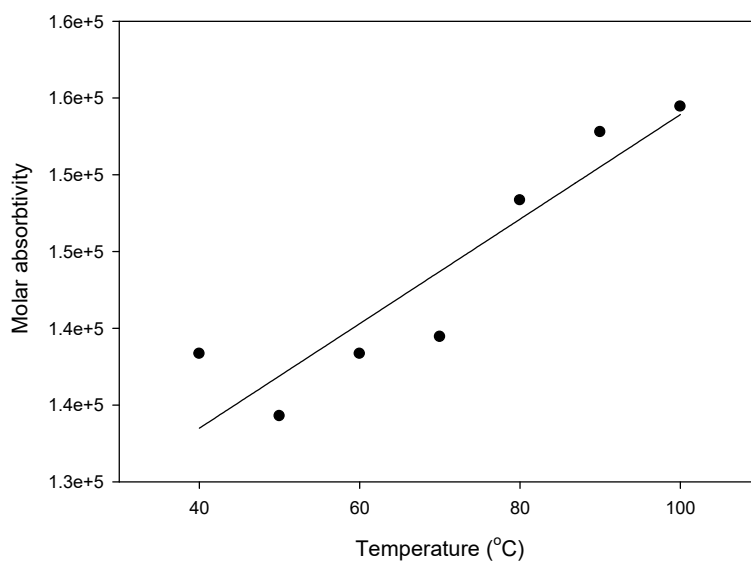

Figure 8. Temperature dependence of the apparent molar absorptivity (ε) of the I6/A SMHBC in the toluene solvent.

4. Conclusions

In the present study, two new types of SMHBLCs complexes were prepared and experimentally and theoretically investigated. Isophthalic acid (A) and terephthalic acid (B) were taken as the proton-donor, while the proton-acceptor was 4-(4-(hexyloxyphenylimino)methyl) phenyl nicotinate (I6).The H-bonding interaction was confirmed through the Fermi bands by FT-IR spectroscopy. Mesophase behavior was estimated by DSC and phases identified by POM. The photophysical studies were carried out by UV-spectroscopic measurements, and computational studies were established through DFT calculations. The results revealed the following:

1. The isophthalic acid complex (I6/A) exhibited an induced enantiotropic SmA phase with a broad range of stability followed by the N mesophase.
2. The terephthalic acid complex (I6/B) was shown to possess only the nematic phase.
3. The SMHBCs of the isophthalic and terephthalic acids were neither linear nor co-planar in W- and U-shaped geometrical structures, respectively.
4. The U-shaped geometry of the terephthalic acid was more stable than that of the W-shaped (I6/A) by 2.6 kcal mol^{-1}.
5. The H-bonded complex derived from the isophthalic A was softer than that from its isomer B.
6. The orientations of the two carboxylic groups of the acid highly affected the direction and mapping of the charge distribution, consequently explaining the enhancement of the induced SmA mesophase for the I6/A complex.

References

1. Beharry, A.A.; Woolley, G.A. Azobenzene photoswitches for biomolecules. *Chem. Soc. Rev.* **2011**, *40*, 4422–4437. [CrossRef] [PubMed]
2. Zhang, B.-Y.; Meng, F.-B.; Tian, M.; Xiao, W.-Q. Side-chain liquid-crystalline polysiloxanes containing ionic mesogens and cholesterol ester groups. *React. Funct. Polym.* **2006**, *66*, 551–558. [CrossRef]
3. laasar, M.; Tschierske, C.; Prehm, M. Hydrogen-bonded supramolecular complexes formed between isophthalic acid and pyridine-based derivatives. *Liq. Cryst.* **2011**, *38*, 925–934. [CrossRef]
4. Ahmed, H.; Naoum, M. Mesophase behaviour of azobenzene-based angular supramolecular hydrogen-bonded liquid crystals. *Liq. Cryst.* **2016**, *43*, 222–234. [CrossRef]
5. Naoum, M.M.; Fahmi, A.A.; Refaie, A.A.; Alaasar, M.A. Novel hydrogen-bonded angular supramolecular liquid crystals. *Liq. Cryst.* **2012**, *39*, 47–61. [CrossRef]
6. Naoum, M.; Fahmi, A.; Alaasar, M. Supramolecular hydrogen-bonded liquid crystals formed from 4-(4′-pyridylazophenyl)-4 ″-alkoxy benzoates and 4-substituted benzoic acids. *Mol. Cryst. Liq. Cryst.* **2008**, *487*, 74–91. [CrossRef]
7. Naoum, M.; Fahmi, A.; Alaasar, M. Supramolecular liquid crystals induced by hydrogen-bonding interactions between non-mesomorphic compounds. I. 4-(4′-Pyridylazophenyl)-4″-substituted benzoates and 4-substituted benzoic acids. *Mol. Cryst. Liq. Cryst.* **2009**, *506*, 22–33. [CrossRef]
8. Naoum, M.M.; Fahmi, A.G.A.; Almllal, W.A. Supramolecular liquid crystals induced by hydrogen-bonding interactions between non-mesomorphic compounds. II. Effect of lateral substitution. *Mol. Cryst. Liq. Cryst.* **2010**, *518*, 109–128. [CrossRef]

9. Ahmed, H.; Hagar, M.; Alhaddad, O. Mesomorphic and geometrical orientation study of the relative position of fluorine atom in some thermotropic liquid crystal systems. *Liq. Cryst.* **2019**, *47*, 404–413. [CrossRef]

10. Prasad, S.K.; Nair, G.G.; Hegde, G. Dynamic self-assembly of the liquid-crystalline smectic A phase. *Adv. Mater.* **2005**, *17*, 2086–2091. [CrossRef]

11. Tanaka, D.; Ishiguro, H.; Shimizu, Y.; Uchida, K. Thermal and photoinduced liquid crystalline phase transitions with a rod–disc alternative change in the molecular shape. *J. Mater. Chem.* **2012**, *22*, 25065–25071. [CrossRef]

12. Alaasar, M.; Poppe, S.; Tschierske, C. Photoresponsive halogen bonded polycatenar liquid crystals. *J. Mol. Liq.* **2019**, *277*, 233–240. [CrossRef]

13. Pintre, I.C.; Serrano, J.L.; Ros, M.B.; Martínez-Perdiguero, J.; Alonso, I.; Ortega, J.; Folcia, C.L.; Etxebarria, J.; Alicante, R.; Villacampa, B. Bent-core liquid crystals in a route to efficient organic nonlinear optical materials. *J. Mater. Chem.* **2010**, *20*, 2965–2971. [CrossRef]

14. Yang, P.C.; Liu, J.H. Synthesis and characterization of novel photoisomerizable liquid crystalline polymers containing cinnamoyl groups. *J. Polym. Sci. Part A Polym. Chem.* **2008**, *46*, 1289–1304. [CrossRef]

15. Kelker, H.; Scheurle, B. A liquid-crystalline (nematic) phase with a particularly low solidification point. *Angew. Chem. Int. Ed.* **1969**, *8*, 884–885. [CrossRef]

16. Ghosh, T.; Lehmann, M. Recent advances in heterocycle-based metal-free calamitics. *J. Mater. Chem. C* **2017**, *5*, 12308–12337. [CrossRef]

17. Carli, J.T.; Lindberg, C.D.; Heltne, M.D.; Bornowski, E.C.; John, E.A.; Wiegel, K.N. Supramolecular main-chain liquid crystalline polymers with competitive hydrogen bonding: Inclusion of structurally analogous hydrogen bond acceptors and the effects on liquid crystallinity. *Mol. Cryst. Liq. Cryst.* **2017**, *656*, 83–88. [CrossRef]

18. Mallia, V.A.; George, M.; Das, S. Photochemical phase transition in hydrogen-bonded liquid crystals. *Chem. Mater.* **1999**, *11*, 207–208. [CrossRef]

19. Nafee, S.S.; Ahmed, H.A.; Hagar, M. New architectures of supramolecular H-bonded liquid crystal complexes based on dipyridine derivatives. *Liq. Cryst.* **2020**, 1–14. [CrossRef]

20. Kato, T.; Adachi, H.; Fujishima, A.; Fréchet, J.M. Self-assembly of liquid crystalline complexes having angular structures through intermolecular hydrogen bonding. *Chem. Lett.* **1992**, *21*, 265–268. [CrossRef]

21. Gimeno, N.; Ros, M.B.; Serrano, J.L.; de la Fuente, M.R. Hydrogen-bonded banana liquid crystals. *Angew. Chem. Int. Ed.* **2004**, *43*, 5235–5238. [CrossRef] [PubMed]

22. Ahmed, H.; Hagar, M.; Alaasar, M.; Naoum, M. Wide nematic phases induced by hydrogen-bonding. *Liq. Cryst.* **2019**, *46*, 550–559. [CrossRef]

23. Ahmed, H.A.; Hagar, M.; Alhaddad, O.A. Phase behavior and DFT calculations of laterally methyl supramolecular hydrogen-bonding complexes. *Crystals* **2019**, *9*, 133. [CrossRef]

24. Ahmed, H.; Hagar, M.; Aljuhani, A. Mesophase behavior of new linear supramolecular hydrogen-bonding complexes. *RSC Adv.* **2018**, *8*, 34937–34946. [CrossRef]

25. Al-Mutabagani, L.A.; Alshabanah, L.A.; Ahmed, H.A.; Hagar, M.; Al-Ola, K.A.A. New symmetrical U-and wavy-shaped supramolecular H-bonded systems; geometrical and mesomorphic approaches. *Molecules* **2020**, *25*, 1420. [CrossRef]

26. Dave, J.S.; Menon, M. Azomesogens with a heterocyclic moiety. *Bull. Mater. Sci.* **2000**, *23*, 237–238. [CrossRef]

27. Abberley, J.P.; Killah, R.; Walker, R.; Storey, J.M.; Imrie, C.T.; Salamończyk, M.; Zhu, C.; Gorecka, E.; Pociecha, D. Heliconical smectic phases formed by achiral molecules. *Nat. Commun.* **2018**, *9*, 1–7.

28. Paterson, D.A.; Crawford, C.A.; Pociecha, D.; Walker, R.; Storey, J.M.; Gorecka, E.; Imrie, C.T. The role of a terminal chain in promoting the twist-bend nematic phase: The synthesis and characterisation of the 1-(4-cyanobiphenyl-4′-yl)-6-(4-alkyloxyanilinebenzylidene-4′-oxy) hexanes. *Liq. Cryst.* **2018**, *45*, 2341–2351. [CrossRef]

29. Abdullah Alshabanah, L.; Al-Mutabagani, L.A.; Ahmed, H.A.; Hagar, M. Induced wide nematic phase by seven-ring supramolecular H-bonded systems: Experimental and computational evaluation. *Molecules* **2020**, *25*, 1694. [CrossRef]

30. Ahmed, H.; Hagar, M.; Alhaddad, O. New chair shaped supramolecular complexes-based aryl nicotinate derivative; mesomorphic properties and DFT molecular geometry. *RSC Adv.* **2019**, *9*, 16366–16374. [CrossRef]

31. Alhaddad, O.; Ahmed, H.; Hagar, M. Experimental and theoretical approaches of new nematogenic chair architectures of supramolecular H-bonded liquid crystals. *Molecules* **2020**, *25*, 365. [CrossRef] [PubMed]

32. Nafee, S.S.; Hagar, M.; Ahmed, H.A.; El-Shishtawy, R.M.; Raffah, B.M. The synthesis of new thermal stable schiff base/ester liquid crystals: A computational, mesomorphic, and optical study. *Molecules* **2019**, *24*, 3032. [CrossRef] [PubMed]

33. Ahmed, N.H.S.; Saad, G.R.; Ahmed, H.A.; Hagar, M. New wide-stability four-ring azo/ester/Schiff base liquid crystals: Synthesis, mesomorphic, photophysical, and DFT approaches. *RSC Adv.* **2020**, *10*, 9643–9656. [CrossRef]

34. Alnoman, R.; Ahmed, H.A.; Hagar, M. Synthesis, optical, and geometrical approaches of new natural fatty acids' esters/Schiff base liquid crystals. *Molecules* **2019**, *24*, 4293. [CrossRef] [PubMed]

35. Setia, S.; Sidiq, S.; De, J.; Pani, I.; Pal, S.K. Applications of liquid crystals in biosensing and organic light-emitting devices: Future aspects. *Liq. Cryst.* **2016**, *43*, 2009–2050. [CrossRef]

36. Nayek, P.; Ghosh, S.; Roy, S.; Majumder, T.P.; Dabrowski, R. Electro-optic and dielectric investigations of a perfluorinated compound showing orthoconic antiferroelectric liquid crystal. *J. Mol. Liq.* **2012**, *175*, 91–96. [CrossRef]

37. Frisch, M.; Trucks, G.; Schlegel, H.B.; Scuseria, G.; Robb, M.; Cheeseman, J.; Scalmani, G.; Barone, V.; Mennucci, B.; Petersson, G. *Gaussian 09, Revision A. 02*; Gaussian Inc.: Wallingford, CT, USA, 2009; p. 200.

38. Dennington, R.; Keith, T.; Millam, J. *GaussView, Version 5*; Semichem Inc.: Shawnee Mission, KS, USA, 2009.

39. Chen, H.; Liu, Y.; Gong, T.; Wang, L.; Zhao, K.; Zhou, S. Use of intermolecular hydrogen bonding to synthesize triple-shape memory supermolecular composites. *RSC Adv.* **2013**, *3*, 7048–7056. [CrossRef]

40. Weinhold, F. Resonance character of hydrogen-bonding interactions in water and other H-bonded species. *Adv. Protein Chem.* **2005**, *72*, 121–155.

41. Cleland, W.; Kreevoy, M.M. Low-barrier hydrogen bonds and enzymic catalysis. *Science* **1994**, *264*, 1887–1890. [CrossRef]

42. Lizu, M.; Lutfor, M.; Surugau, N.; How, S.; Arshad, S.E. Synthesis and characterization of ethyl cellulose–based liquid crystals containing azobenzene chromophores. *Mol. Cryst. Liq. Cryst.* **2010**, *528*, 64–73. [CrossRef]

43. Martinez-Felipe, A.; Cook, A.G.; Abberley, J.P.; Walker, R.; Storey, J.M.; Imrie, C.T. An FT-IR spectroscopic study of the role of hydrogen bonding in the formation of liquid crystallinity for mixtures containing bipyridines and 4-pentoxybenzoic acid. *RSC Adv.* **2016**, *6*, 108164–108179. [CrossRef]

44. Martínez-Felipe, A.; Imrie, C.T. The role of hydrogen bonding in the phase behaviour of supramolecular liquid crystal dimers. *J. Mol. Struct.* **2015**, *1100*, 429–437. [CrossRef]

45. Ghanem, A.; Noel, C. FTIR investigation of two alkyl-p-terphenyl-4, 4''-dicarboxylates in their crystalline, smectic and isotropic phases. *Mol. Cryst. Liq. Cryst.* **1987**, *150*, 447–472. [CrossRef]

46. Paterson, D.A.; Martínez-Felipe, A.; Jansze, S.M.; TM Marcelis, A.; MD Storey, J.; Imrie, C.T. New insights into the liquid crystal behaviour of hydrogen-bonded mixtures provided by temperature-dependent FTIR spectroscopy. *Liq. Cryst.* **2015**, *42*, 928–939. [CrossRef]

47. Walker, R.; Pociecha, D.; Abberley, J.; Martinez-Felipe, A.; Paterson, D.; Forsyth, E.; Lawrence, G.; Henderson, P.; Storey, J.; Gorecka, E. Spontaneous chirality through mixing achiral components: A twist-bend nematic phase driven by hydrogen-bonding between unlike components. *Chem. Commun.* **2018**, *54*, 3383–3386. [CrossRef]

48. Nafee, S.S.; Hagar, M.; Ahmed, H.A.; Alhaddad, O.; El-Shishtawy, R.M.; Raffah, B.M. New two rings Schiff base liquid crystals; ball mill synthesis, mesomorphic, Hammett and DFT studies. *J. Mol. Liq.* **2020**, *299*, 112161. [CrossRef]

49. Nafee, S.S.; Ahmed, H.; Hagar, M. Theoretical, experimental and optical study of new thiophene-based liquid crystals and their positional isomers. *Liq. Cryst.* **2020**, 1–12. [CrossRef]

50. Hagar, M.; Ahmed, H.; Alhaddad, O. New azobenzene-based natural fatty acid liquid crystals with low melting point: Synthesis, DFT calculations and binary mixtures. *Liq. Cryst.* **2019**, *46*, 2223–2234. [CrossRef]

51. Passchier, A.; Christian, J.D.; Gregory, N.W. The ultraviolet-visible absorption spectrum of bromine between room temperature and 440°. *J. Phys. Chem.* **2002**, *71*, 937–942. [CrossRef]